The current issue and full text archive of this journal is available at
www.emeraldinsight.com/0961-5539.htm

Received 5 December 2005
Revised 2 January 2007
Accepted 12 March 2007

A numerical model for calculating the vaporization rate of a fuel droplet exposed to a convective turbulent airflow

Maher M. Abou Al-Sood and Madjid Birouk
Department of Mechanical and Manufacturing Engineering, University of Manitoba, Winnipeg, Canada

Abstract

Purpose – The purpose of this paper is to develop a three-dimensional (3D) numerical model capable of predicting the vaporization rate of a liquid fuel droplet exposed to a convective turbulent airflow at ambient room temperature and atmospheric pressure conditions.

Design/methodology/approach – The 3D Reynolds-Averaged Navier-Stokes equations, together with the mass, species, and energy conservation equations were solved in Cartesian coordinates. Closure for the turbulence stress terms for turbulent flow was accomplished by testing two different turbulence closure models; the low-Reynolds number (LRN) k-ε and shear-stress transport (SST). Numerical solution of the resulted set of equations was achieved by using blocked-off technique with finite volume method.

Findings – The present predictions showed good agreement with published turbulent experimental data when using the SST turbulence closure model. However, the LRN k-ε model produced poor predictions. In addition, the simple numerical approach employed in the present code demonstrated its worth.

Research limitations/implications – The present study is limited to ambient room temperature and atmospheric pressure conditions. However, in most practical spray flow applications droplets evaporate under ambient high-pressure and a hot turbulent environment. Therefore, an extension of this study to evaluate the effects of pressure and temperature will make it more practical.

Originality/value – It is believed that the numerical code developed is of great importance to scientists and engineers working in the field of spray combustion. This paper also demonstrated for the first time that the simple blocked-off technique can be successfully used for treating a droplet in the flow calculation domain.

Keywords Modelling, Numerical analysis, Turbulent flow, Vaporization

Paper type Research paper

Nomenclature

A = cross section area (m^2)
D = diffusion conductance
h_{evap} = latent heat of vaporization
I = turbulence intensity ($\sqrt{\overline{u'^2}}/U_\infty$)
K = turbulence kinetic energy (m^2/s^2)
K = evaporation rate (mm^2/s)
L = length of the computational domain (m)
$\dot{m}$ = mass flow rate (kg/s)
$\dot{m}''_{evap}$ = evaporated mass flux (kg/m^2)
Pe = Peclet number
Pr = Prandtl number

The authors thank the Natural Sciences and Engineering Research Council of Canada (NSERC) and the University of Manitoba for their financial support.

International Journal of Numerical Methods for Heat & Fluid Flow
Vol. 18 No. 2, 2008
pp. 146-159
© Emerald Group Publishing Limited
0961-5539
DOI 10.1108/09615530810846301

p = pressure (Pa)
Re = Reynolds number
S_ϕ = source term ($S_\phi = S_C + S_P\phi$)
t = time (s)
U_∞ = freestream mean velocity (m/s)
U_d = droplet velocity (m/s)
u = velocity component in x-direction (m/s)
v = velocity component in y-direction (m/s)
w = velocity component in z-direction (m/s)
Y_f = fuel mass fraction

Greek letters
ε = turbulence dissipation rate (m^2/s^3)
ω = specific rate of turbulence dissipation
Φ = diffusion parameter ($u, v, w, p, k, \varepsilon$ or ω)
μ = molecular viscosity (Pa s)
μ_t = turbulence viscosity (Pa s)
ρ = density (kg/m^3)
α = convection weighting factor
β = diffusion weighting factor
Γ = generalized diffusion coefficient
λ = thermal conductivity (W/m k)
τ = shear stress
Δx = control volume length in x-direction
Δy = control volume length in y-direction
Δz = control volume length in z-direction
δ_{ij} = Kronecker delta

Subscripts
i = Cartesian coordinates x ($i = 1$), y ($i = 2$) or z ($i = 3$)
ij = xy ($ij = 12$), xz ($ij = 13$) or zx ($ij = 31$) plane of the control volume
B = bottom ($i, j, k - 1$) node
E = east ($i + 1, j, k$) node
N = north ($i, j + 1, k$) node
P = center (i, j, k) node
S = south ($i, j - 1, k$) node
T = top ($i, j, k + 1$) node
W = west ($i - 1, j, k$) node
b = control volume bottom ($i, j, k - 1/2$) face
e = control volume east ($i + 1/2, j, k$) face
n = control volume north ($j + 1/2$) face
s = control volume south ($i, j - 1/2, k$) face
t = control volume top ($i, j, k + 1/2$) face
w = control volume west ($i - 1/2, j, k$) face; wall

Introduction

The evaporation of fuel droplets is fundamentally and practically important for many engineering systems. For example, the vaporization rate of liquid fuel is the controlling parameter in liquid-fuelled combustion systems. Therefore, studying and understanding the vaporization of a liquid fuel droplet is a prerequisite for understanding the complex spray flows. A liquid droplet evaporating in a free or forced convective laminar flow received great attention in the last century, which resulted in the establishment of well-accepted correlations for the heat and mass transport rates from a liquid droplet. Much of the credit of this progress goes to the pioneering research work undertaken by Frössling (1938) in the late 1930s and, pursued by Ranz and Marchall (1952) in the late 1950s.

The study of the evaporation of liquid droplets in turbulent flow environments, however, received less attention, and consequently it is still less understood. A review of the open literature revealed that almost all the few published work on the effects of turbulence on the vaporization of droplets in forced convective turbulent flows or in zero-mean velocity turbulent flows are experimental (Gökalp *et al.*, 1992; Birouk *et al.*, 1996; Wu *et al.*, 2001 and references cited therein). To the authors' knowledge only a few attempts were made to develop numerical studies (Park and Farrell, 1990; Masoudi and Sirignano, 2000). Park and Farrell (1990) developed a two-dimensional (2D) numerical model to investigate the effects of turbulent flows on mass transfer from n-hexane droplet having an initial diameter in the range between 100 and 400 μm. Their test conditions included Reynolds number and freestream turbulence intensity, I_∞, in the range from 50 to 200 and from 0 to 50 per cent, respectively. They verified the code by

comparing their results with turbulent convective flows over a sphere. In addition to the fact that their model was a 2D which obviously cannot represent the characteristics of a 3D turbulent flow, a realistic validation of the model was lacking. Recently, Masoudi and Sirignano (2000) introduced a newer approach in an attempt to investigate the role of the largest spatial flow structures on heat and mass transfer to and from an evaporating droplet, respectively. Their approach consisted of placing a vortex in the convective flow upstream of the droplet and solving the three dimensional (3D) Navier-Stokes equations. They reported that the Sherwood (mass transfer) and Nusselt (heat transfer) numbers are higher than their counterparts' axisymmetrical values if the vortex centre is positioned far away from the droplet horizontal axis. Furthermore, the Sherwood and Nusselt numbers values were found to be identical for *n*-heptane, *n*-octane and *n*-decane droplets. This may suggest that their proposed correlations for these numbers could be generalized for a wide range of hydrocarbon fuels.

In the approach adopted by Masoudi and Sirignano (2000), the rate of heat and mass transfer between the convective flow and the droplet were evaluated as a function of a vortex and its position with respect to the droplet. The most recent experimental studies which dealt with the effect of a turbulent convective flow were performed by Gökalp *et al.* (1992) and Wu *et al.* (2001). In both studies, the largest turbulence scale, i.e. integral length scale, was much higher than the droplet initial diameter. Therefore, the effect of turbulence on the droplet vaporization rate was explained in terms of turbulence intensity. The same approach was adopted in the present study to develop a 3D numerical model for predicting the rate of mass transfer (i.e. mass evaporation rate) from a liquid droplet exposed to a convective turbulent flow. The version of the numerical model presented in this paper is limited to ambient room temperature and atmospheric pressure conditions to enable comparing our data with the published experimental data mentioned above. However, an extension of this model which includes high-pressure and hot ambient gas conditions is currently underway and will be presented in subsequent contributions.

Problem description

Consider a liquid droplet with an initial radius r_0 and an initial temperature T_0 immersed into turbulent inert airflow of infinite expanse. The gas phase is described by U_∞, p_∞, T_∞, $Y_{f\infty}$ and I_∞. The physical geometry of the problem with the initial and boundary conditions are shown in Figure 1. The liquid droplet is stationary and

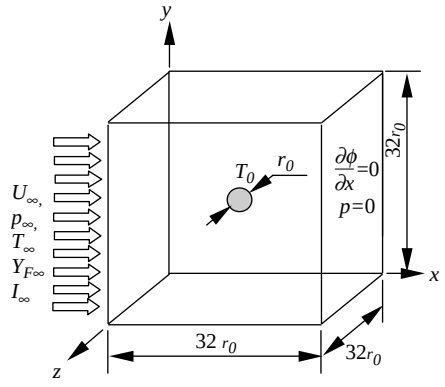

Figure 1.
Schematic of an evaporating droplet exposed to a convective turbulent flow along with initial and boundary flow conditions

immersed at a uniform temperature. Energy in the form of heat is transferred from the gas phase to the liquid phase. A fraction of this energy is used to heat-up the interior of the droplet, and only the remaining fraction of heat is used for droplet's evaporation. Once the droplet surface temperature reaches its steady-state value, all the heat received by the droplet is used for evaporation only. The evaporation of the liquid droplet (i.e. mass transfer) yields a decrease in the droplet radius. The evaporated mass is then diffused and convected away from the droplet surface and hence the gas phase becomes a mixture of fuel vapor and air.

Mathematical formulation

Governing equations and assumptions

The following assumptions are employed in the present model:

- the droplet shape remains spherical since the Weber number is much less than unity;
- the droplet evaporates in inert surroundings;
- the gas phase is steady and incompressible;
- the freestream turbulence is assumed a priori known; and
- radiation and second order effects such as Soret and Dafour effects are assumed negligible.

The governing equations for the gas phase are the Reynolds-Averaged Navier-Stokes, energy and mass species conservation equations, which are given, respectively, as:

$$\frac{\partial \rho}{\partial t} + \frac{\partial}{\partial x_i}(\rho u_i) = 0 \tag{1}$$

$$\frac{\partial}{\partial t}(\rho u_i) + \frac{\partial}{\partial x_j}(\rho u_i u_j) = -\frac{\partial p}{\partial x_i} + \frac{\partial}{\partial x_j}\left(\mu \frac{\partial u}{\partial x_j} - \overline{\rho u_i' u_j'}\right) \tag{2}$$

$$\frac{\partial}{\partial t}(\rho T) + \frac{\partial}{\partial x_j}(\rho u_i T) = \frac{\partial}{\partial x_j}\left(\frac{\mu}{Pr}\frac{\partial T}{\partial x_j} - \overline{\rho u_i' T'}\right) \tag{3}$$

$$\frac{\partial}{\partial t}(\rho Y_{\mathrm{f}}) + \frac{\partial}{\partial x_j}(\rho u_i Y_{\mathrm{f}}) = \frac{\partial}{\partial x_j}\left(\frac{\mu}{Sc}\frac{\partial Y_{\mathrm{f}}}{\partial x_j} - \overline{\rho u_i' Y_{\mathrm{f}}'}\right) \tag{4}$$

Closure for the turbulence stress terms for the gas phase was obtained by testing two different models: low-Reynolds number k-ε of Jones and Launder (1973) and the shear-stress transport (SST) of Menter (1994). Since, the characteristic time for changes in the gas phase, which is the residence time in the neighborhood of the droplet, is much smaller than the droplet lifetime, the quasi-steady gas phase assumption can be employed (Prakash and Sirginano, 1979). Therefore, unsteady terms in the conservation equations are cancelled by making the time interval, in the discretized equation, of the order 10^{30} s. For the liquid phase (i.e. droplet), the governing equations are basically the unsteady continuity, momentum and energy equations, which are given by the equations (1)-(3) shown above but with zero-turbulent terms.

Freestream and gas-liquid interface conditions

The freestream values for velocities, pressure and turbulence quantities were taken at the boundary of the calculation domain, which is about $32r_0$ upstream of the droplet, as $u = U_\infty, v = 0, w = 0, p = p_\infty\, k = k_\infty, \varepsilon = \varepsilon_\infty$ and $\omega = \omega_\infty$. The free stream values for k, ε and ω are estimated from the following relations (Karel, 1998):

$$k_\infty = 1.5(I_\infty \times U_\infty)^2 \tag{5}$$

$$\varepsilon_\infty = c_\mu f_\mu \rho \frac{k_\infty^2}{\mu_{t\infty}} Re \tag{6}$$

$$\omega_\infty = 10\frac{U_\infty}{L} \tag{7}$$

where, $Re = (U_\infty - U_d)d_0/v_\infty$ with $(U_\infty - U_d)$ is the relative velocity, L is the characteristic length of the calculation domain, f_μ is the damping function, and $\mu_{t\infty}$ is the freestream turbulent viscosity which is taken as $\mu_{t\infty} \cong (0.1 - 10)\mu_\infty$ (Karel, 1998).

Conditions at the distinctive gas-liquid interface are obtained by the coupling between the conservation equations in gas and liquid phases as follow:

- *shear stress continuity:*

$$\tau_{ij,g} = \tau_{ij,l} \tag{8}$$

- *tangential velocity continuity:*

$$U_{tan}|_g = U_{tan}|_l = U_s \tag{9}$$

- *normal velocity continuity:*

$$U_{nor}|_l = \left(\frac{\rho_g}{\rho_l}\right) U_{nor}|_g + \left(1 - \frac{\rho_g}{\rho_l}\right)\dot{r} \tag{10}$$

- *temperature continuity:*

$$T_g = T_l = T_s \tag{11}$$

- *energy conservation:*

$$\lambda_{eff}\left.\frac{\partial T}{\partial x_i}\right|_g = \lambda\left.\frac{\partial T}{\partial x_i}\right|_l + \dot{m}''_{evap_i} h_{evap} \tag{12}$$

- *species conservation:*

$$\dot{m}''_{evap_i}(Y_{f,g} - 1) - \rho_g D_{AB,g}\frac{\partial Y_{f,g}}{\partial x_i} = 0 \tag{13}$$

- *conservation of droplet mass:*

$$\dot{r} - = \frac{\sum_{\substack{\text{evaporated}\\ \text{surfaces}}} \dot{m}''_{\ evap_i} A}{4\pi\rho r^2} + \frac{r}{3\rho}\,\frac{d\rho}{dt} \tag{14}$$

where the subscripts g and l denote the variable in the gas side and liquid side at the droplet interface (which is denoted by *s*), respectively; tan and nor denote tangential and normal to the control volume surface, respectively; *ij* denotes the coordinates of shear stress plane, which could be *xy*, *yz* or *zx* depending on the control volume faces being subjected to air flow and, *i* denotes *x*, *y* or *z* coordinates. The symbol $\dot{r}$ denotes the regression rate of the spherical droplet surface, r is the instantaneous droplet radius, A is the surface area of the node subjected to the flow, $Y_{f,g}$ is the fuel mass fraction in the gas phase, $\dot{m}''_{evap}$is the fuel mass flux, h_{evap} is the fuel enthalpy of vaporization, $D_{AB,g}$ is the coefficient of the fuel vapor molecular diffusion into air, λ_{eff} is the effective thermal conductivity.

Numerical solution

Discretization and numerical approach

The set of equations described above for the gas and liquid phases can be conveniently summarized in a general transport equation having the following form:

$$\frac{\partial}{\partial t}(\rho\Phi) + \frac{\partial}{\partial x_j}(\rho u_i \Phi) = \frac{\partial}{\partial x_j}\left\{\Gamma_\phi \frac{\partial \Phi}{\partial x_j}\right\} + S_\Phi \tag{15}$$

the general variable, Φ represents the flow velocity components u, v or w, pressure p, temperature T, mass fraction Y_f or turbulence quantities such as k, ε or ω. In order to solve the complex nonlinear strongly coupled set of governing transport equations, finite volume method was employed (Patankar, 1980). The governing differential equations were integrated over discrete volumes resulting in a set of algebraic equations of the following general form:

$$a_P\Phi_P = a_E\Phi_E + a_W\Phi_W + a_N\Phi_N + a_S\Phi_S + a_T\Phi_T + a_B\phi_B + b_\phi \tag{16}$$

where the coefficients a_P, a_E, a_W, a_N, a_S, a_T, a_B, and b_ϕ are defined as:

$$\left.\begin{aligned} a_P &= a_E + a_W + a_N + a_S + a_T + a_B - S_P\Delta x\Delta y\Delta z \\ b_\phi &= S_C\Delta x\Delta y\Delta z \\ a_E &= \beta_e D_e + \dot{m}_e\alpha_e - \dot{m}_e/2 \\ a_W &= \beta_w D_w + \dot{m}_w\alpha_w + \dot{m}_w/2 \\ a_N &= \beta_n D_n + \dot{m}_n\alpha_n - \dot{m}_n/2 \\ a_S &= \beta_s D_s + \dot{m}_s\alpha_s + \dot{m}_s/2 \\ a_T &= \beta_t D_t + \dot{m}_t\alpha_e - \dot{m}_t/2 \\ a_B &= \beta_b D_b + \dot{m}_b\alpha_b + \dot{m}_b/2 \end{aligned}\right\} \tag{16.1}$$

and the subscripts P, E, W, N, S, T and B refer to the center point of the central, east, west, north, south, top and bottom control volumes. Whereas e, w, n, s, t and b refer to east, west, north, south, top and bottom face of the central control volume *P*. S_P and S_C are the coefficients of the linearized source term, which is given as $S_\Phi = S_C + S_P\Phi$. Some of the parameters appeared in the above equation (16.1) are given as:

$$\left.\begin{aligned} D_{\mathrm{i}} &= 2\Gamma_{\mathrm{i}}A_{\mathrm{i}}/(\Delta x_{\mathrm{I}} + \Delta x_{\mathrm{P}}) \\ \Gamma_{\mathrm{i}} &= \Gamma_{\mathrm{P}}\Gamma_{\mathrm{I}}/[\Gamma_{\mathrm{I}}\Gamma_{\mathrm{P}} + (1-f_{\mathrm{i}})\Gamma_{\mathrm{I}}] \\ f_{\mathrm{i}} &= \frac{(\Delta x_j)_{\mathrm{I}}}{(\Delta x_j)_{\mathrm{I}}+(\Delta x_j)_{\mathrm{P}}} \\ \alpha_{\mathrm{i}} &= \frac{1}{2}\times\frac{(Pe)_{\mathrm{i}}^2}{5+(Pe)_{\mathrm{i}}^2} \\ \beta_{\mathrm{i}} &= \frac{1+0.005(Pe)_{\mathrm{i}}^2}{1+0.05(Pe)_{\mathrm{i}}^2} \\ (Pe)_{\mathrm{i}} &= \frac{\dot{m}_{\mathrm{i}}}{D_{\mathrm{i}}} \end{aligned}\right\} \tag{16.2}$$

where $\Delta x_j = \Delta x$ for $j = 1$, $\Delta x_j = \Delta y$ for $j = 2$ and $\Delta x_j = \Delta z$ for $j = 3$, respectively, f_{i} is the ratio of the neighborhood node length to the total length of neighborhoods and central nodes in x, y or z direction, with $f = 0.5$ if the grid is uniform. The subscript I in equation (16.2) denotes E, W, N, S, T or B and, and subscript i denotes e, w, n, s, t or b which are defined above.

In working numerically with the so-called primitive variables u, v, w and p, the absence of an explicit equation for pressure presents a difficulty. This difficulty was overcome by using SIMPLEC approach (van Doormall and Raithby, 1984) in which an expression in the form of equation (16) was derived for the pressure through a combination of the continuity and momentum equations. The ultimate goal was to develop a pressure field such that the resulting velocity field must satisfy the continuity equation for every control volume in the calculation domain. The solution of the set of linearized algebraic equations in the form of equation (16) was accomplished by using 3D strongly implicit procedure developed by Leister and Perić (1994). Iterative sweeps of the solution domain (gas phase or liquid phase) were continued until one of the two imposed conditions was achieved; either the assigned maximum number of iterations was exceeded or the range-normalized relative errors of the diffusion parameters (u, v, w, p, k, ε or ω) were satisfied for each control volume as:

$$\left|\frac{\Phi^{n+1} - \Phi^{n}}{\Phi_{\max} - \Phi_{\min}}\right| \leq \zeta_{\Phi} \tag{17}$$

where $\Phi_{\max}$ and $\Phi_{\min}$ are the maximum and minimum Φ^{n+1} values. ζ_{Φ} is taken to be 10^{-4} for all quantities.

Numerical treatment of droplet in the calculation domain and solution procedure

To numerically solve for the liquid phase (droplet) and the gas phase a simple technique, called blocked-off treatment, is employed. Analysis of the literature revealed that this technique has been successfully applied to various simple and complex different flow and geometry configurations (see, for example, Byun *et al.*, 2003; Borjini *et al.*, 2003; Consalvi and Lraud, 2003; Zhou and Liu, 2004, and references cited therein). To the authors' best knowledge, apart from a very recent study by Birouk and Abou Al-Sood (2006), no attempt has been made to employ blocked-off technique for a flow over spherical object.

The blocked-off treatment of a droplet immersed in the computational domain in the Cartesian coordinates is schematically shown in Figure 2. Using the block-off technique to solve for the gas or liquid phases requires switching the active and inactive (i.e. blocked) control volumes between the two regions. When solving for the gas phase, the control volumes forming the liquid phase (droplet) are kept inactive. Similarly, when solving for the liquid phase, the control volumes forming the liquid phase are active and those forming the gas phase are kept inactive. For the inactive control volumes, the transport parameters represented in the general form by $\Phi_{P,desired}$ maintain their previous values before they become inactive. Note that this technique makes the surface of a droplet looks like stair steps as shown in Figure 2. Although the computation was executed for the entire calculation domain, only the solution within the active control volumes was meaningful. The desired value for a given parameter in the inactive control volumes can be obtained by assigning large values to the source term in the discretization equation (16). For example, setting S_C and S_P in equation (16.1) for the internal grid points in the inactive zone as:

$$\left.\begin{aligned} S_C &= 10^{30}\Phi_{P,desired} \\ S_P &= -10^{30} \end{aligned}\right\} \tag{18}$$

where 10^{30} denotes a number large enough to make the other terms in discretization equation negligible. Thus, equation (16.1) becomes $S_C + S_P\Phi_P = 0$, so that $\Phi_P = -S_C/S_P = \Phi_{P,desired}$.

The calculation domain was chosen to be a cube of $32r_0 \times 32r_0 \times 32r_0$, where r_0 is the droplet initial radius. The choice of the length of the cube is based on the suggestions made by Sundararajan and Ayyaswamy (1984) who indicated that the freestream conditions must be at least ten times the droplet radius. This is because the location of the freestream conditions may affect the numerical solution as the pressure correction equation is elliptical in nature. The computation domain was divided into control volumes and the droplet was generated at the centre. Figure 1 shows the computational domain and the boundary conditions as the left and right

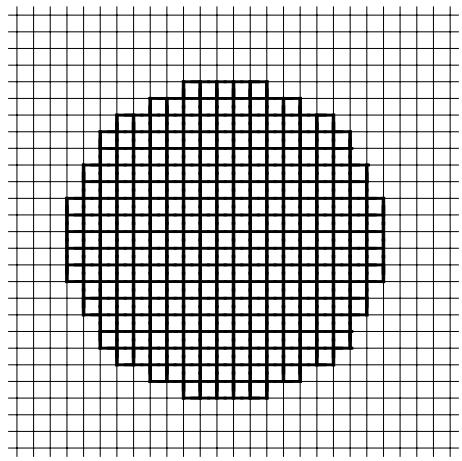

Figure 2.
Cartesian-based blocked-off treatment of an evaporating droplet immersed in the computational domain

faces are inflow and outflow boundary conditions, respectively. The other faces; north, south, top and bottom were taken as the wall boundary conditions. In the present analysis, the Cartesian grid in the calculation domain consisted of $60 \times 60 \times 60$. Since, the gradients around the droplets were large, a very fine grid of $40 \times 40 \times 40$ was used in the domain $2r$ (where r is the instantaneous droplet radius) from the sphere centre in all directions, as shown schematically in Figure 1. Preliminary tests were carried out to render to results independent on the grid.

Results and discussions

The results presented herein are mainly for validating the 3D numerical model we developed in this paper. The test conditions are limited to those reported in Table I. These conditions are deliberately chosen to match those of published results so that a comparison can be made.

The accuracy of the present numerical model is first checked by verifying the level of error involved in the calculation of the volume and surface area of the droplet by using the blocked-off technique. This is because the blocked-off technique cannot configure the exact spherical shape of the droplet, as can be seen in Figure 2. Thus, we decided to test the accuracy of this technique by comparing the instantaneous volume and surface area of the evaporating droplet obtained by the calculation technique (i.e. blocked-off treatment) versus those computed by using the theoretical expression as $V_d = \pi d^3/6$ and $A_d = 0.5\pi d^2$, respectively, where the droplet diameter ($d = 2r$) is obtained from equation (14). The blocked-off technique approximates the droplet as the sum of 1,436 control volumes. These control volumes have a total of 8,616 surfaces/faces (each control volume has six surfaces) but only 4,190 surfaces are subjected to flow and eventually represent the outer surface of droplet. Note that the number of control volumes and surfaces are kept constant throughout whereas their dimensions change (Abou Al-Sood, 2006). The results are shown in Figure 3. This figure shows that the difference between the two methods is almost unnoticeable, less than 1 per cent, indicating the accuracy of the blocked-off technique. We found that the error induced by the blocked-off technique can be minimized by making an adequately fine grid in the $2r$ calculation domain.

The current 3D model is validated first by comparing the present numerical predictions against the existing published experimental and numerical laminar data. The laminar predictions of the present code were obtained by assigning a value of zero to the freestream turbulence intensity in the numerical code. Figure 4 shows a typical variation of the time-history of the squared normalized 1.18 mm diameter of n-heptane droplet in a forced convective laminar flow having a streamwise mean velocity of $U_{\infty=}6$ m/s. This figure shows that the present predictions agree reasonably well with the published numerical data (Zhang, 2003) and almost perfectly with experimental data (Gökalp *et al.*, 1988).

Figures 5(a) shows the variation of the surface temperature of n-heptane droplet versus the evaporation time for different turbulence intensities. As expected, this figure exhibits two distinct regions; transient and steady state. At any given freestream flow conditions, the transient region shows a rapid increase in the droplet surface

Flow	d_0 (mm)	U_∞ (m/s)	I_∞ (per cent)	p_∞ (atm)	T_∞ (K)	Re_∞
Laminar	1.18, 1.50	6.0, 1.0	0.0	1.0	297	472
Turbulent	1.50	1.0	1.0-60	1.0	300	~100

Table I.
Test conditions

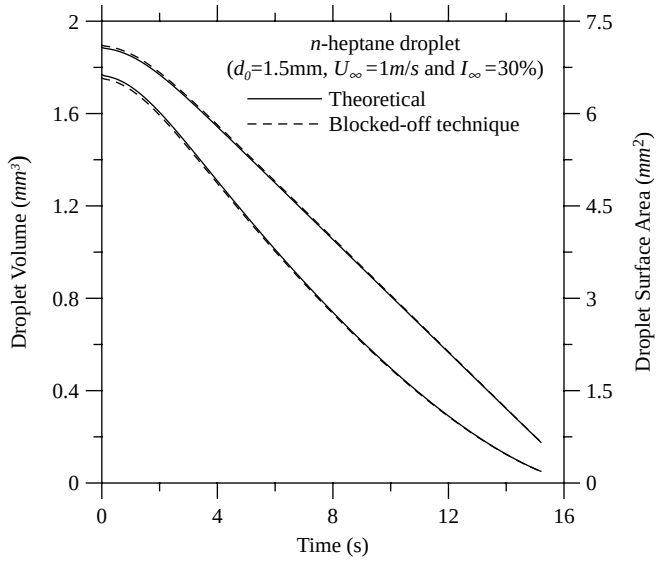

Figure 3.
Time-history of *n*-heptane droplet volume and evaporating surface area

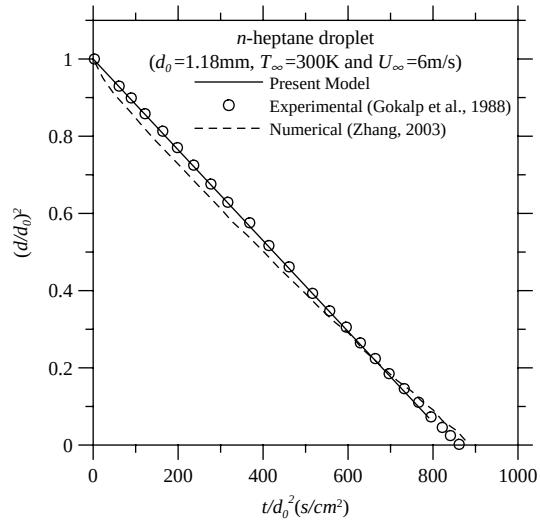

Figure 4.
Time-history of the squared normalized diameter for *n*-heptane droplet in a convective laminar flow

temperature until it reaches a constant temperature, i.e. wet-bulb temperature. During the transient lifetime of the droplet, most of the heat transferred to the liquid phase is used to heat up the liquid droplet. The steady-state region is characterized by a constant temperature, i.e. the wet-bulb temperature, which indicates that all the heat transferred to the liquid droplet is used only for evaporating the droplet. More importantly, the Figure 5(a) and (b) reveals that the droplet heat-up period decreases as the freestream turbulence intensity increases, indicating an increase of the rate of heat transfer to the droplet as a result of an increase in the turbulence intensity. The only

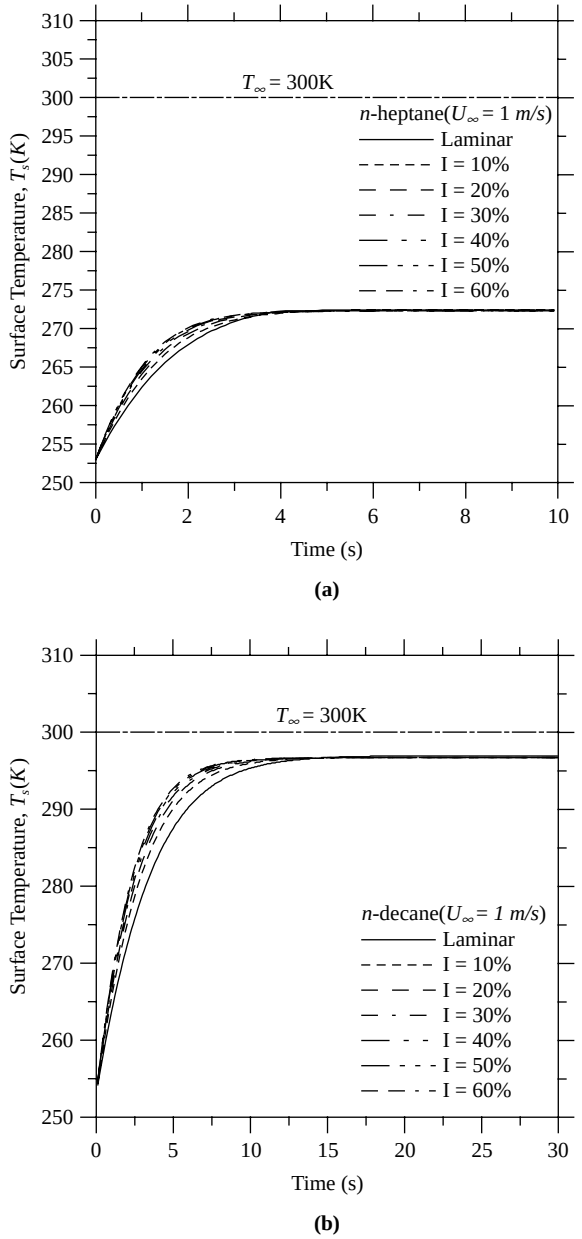

Figure 5.
(a) Time-history of *n*-heptane droplet surface temperature for various freestream turbulence intensities; (b) time-history of *n*-decane droplet surface temperature for various freestream turbulence intensities

noticeable difference between the two droplets is that the surface temperature of *n*-heptane is less than that of *n*-decane. This is due to the difference in the amount of heat stored inside the droplet, which is directly proportional to the droplet boiling temperature that is higher for *n*-decane.

Figure 6 shows the time-history of the squared normalized diameter of *n*-decane droplet versus the normalized evaporation time for quiescent and laminar flow, as well as for various flow turbulence intensities. The droplet life time was terminated when 97.3 per cent of the droplet has evaporated, however, only the initial portion of the laminar and quiescent curves was shown in Figure 6 to enable observing the effect of turbulence. After the elapse of the heating-up period the squared droplet diameter appears to follow a linear variation with the evaporation time obeying the famous d^2-law. Moreover, this figure clearly shows that turbulence decreases the life time of the liquid droplet yielding an increase in the mass transfer (the evaporation rate) from the droplet. The same scenario is seen with *n*-heptane droplet but not shown here to avoid duplication. The predicted vaporization rate of *n*-heptane and *n*-decane droplets under turbulent flow conditions were compared with published experimental data (Wu *et al.*, 2001), as shown in Figure 7. Clearly, the present numerical predictions obtained by using the SST closure model agree reasonably well with their counterparts' experimental data within the experimental error. However, the low-Reynolds k-ε model produced unsatisfactory results, as it overpredicts the vaporization rate of the droplets. This is due to the fact that the value of the calculated turbulent viscosity based on the low-Reynolds k-ε model is slightly higher than that based on the SST model, which in turn yields a higher mass evaporation according to equation (12). Recall that the effective thermal conductivity term appearing in equation (12) increases with turbulent viscosity.

Summary

Blocked-off technique with the finite volume method is used to develop a three dimensional numerical model designed to predict the evaporation rate of a liquid (hydrocarbons) fuel droplet exposed to a forced convective turbulent flow at atmospheric pressure and room temperature conditions. Although, the blocked-off technique in the Cartesian coordinates as applied to a flow over a spherical object (sphere or droplet) cannot

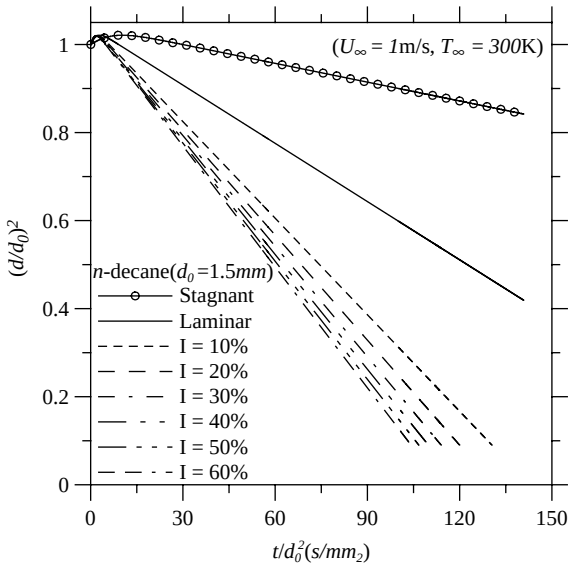

Figure 6.
Time-history of the squared normalized diameter for *n*-decane droplet for different flow conditions

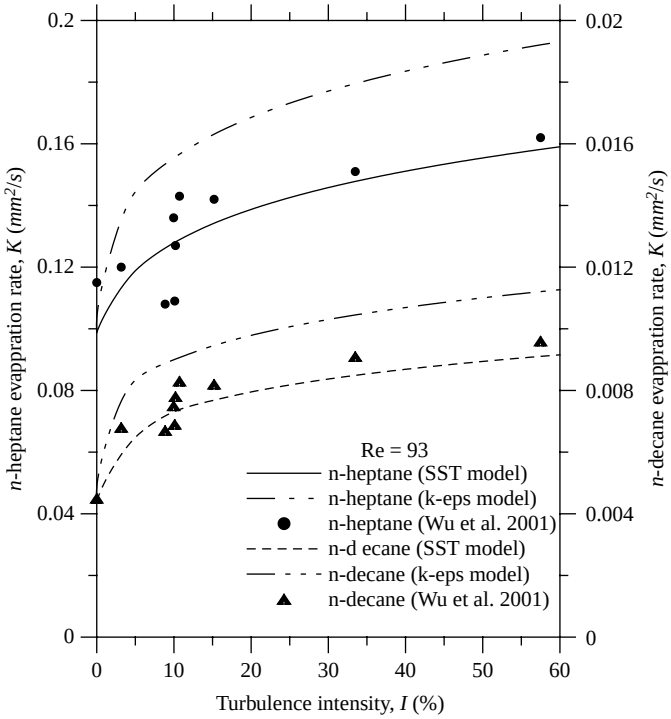

Figure 7.
Variation of the evaporation rate of *n*-heptane and *n*-decane droplets versus freestream turbulence intensity

configure the exact shape of the droplet, the induced error can be reduced substantially by increasing the number of grids in the droplet's region. The developed numerical code based on the SST model predicted reasonably well the vaporization rate of hydrocarbons fuel droplets. Whereas, the same numerical code but based on the low-Reynolds k-ε turbulence closure model produced unsatisfactory predictions.

References

Abou Al-Sood, M.M. (2006), "Simulation and modeling of a droplet evaporating in a turbulent flow", PhD thesis, University of Manitoba, Winnipeg.

Birouk, M. and Abou Al-Sood, M.M. (2006), "Numerical study of sphere drag coefficient in turbulent flow at low Reynolds number", *Numerical Heat Transfer A*, Vol. 51 No. 1, pp. 39-57.

Birouk, M., Chauveau, C., Sarh, B., Quilgars, A. and Gökalp, I. (1996), "Turbulence effects on the vaporization of monocomponent single droplets", *Combustion Science and Technology*, Vol. 113/114, pp. 413-28.

Borjini, M.N., Farahat, H. and Radhouani, M.S. (2003), "Analysis of radiative heat transfer in a partitioned idealized furnace", *Numerical Heat Transfer A*, Vol. 44, pp. 199-218.

Byun, D.Y., Baek, S.W. and Kim, M.Y. (2003), "Investigation of radiative heat transfer in complex geometries using blocked-off, multiblock, and embedded boundary treatments", *Numerical Heat Transfer A*, Vol. 43 No. 8, pp. 807-25.

Consalvi, J.L. and Lraud, J.C. (2003), "Method for computing the interaction of fire environment and internal solid boundaries", *Numerical Heat Transfer A*, Vol. 43, pp. 777-805.

Frössling, N. (1938), "Gerlands beitr", *Geophys.*, Vol. 52, pp. 170-5.

Gökalp, I., Chauveau, C. and Richard, J.R. (1988), "Observation on the low temperature vaporization and envelope or wake flame burning of *n*-heptane droplet at reduced gravity during parabolic flights", *Proceeding of the Combustion Institute*, Vol. 22, pp. 2027-35.

Gökalp, I., Chauveau, C., Simon, O. and Chesneau, X. (1992), "Mass transfer from liquid fuel droplets in turbulent flow", *Combustion and Flame*, Vol. 89, pp. 286-98.

Jones, W.P. and Launder, B.E. (1973), "The calculation of low-Reynolds-number phenomena with a two-equation model of turbulence", *International Journal of Heat and Mass Transfer*, Vol. 16, pp. 1119-30.

Karel, L.D. (1998), "Recent experience with different turbulence models applied to the calculation of flow over aircraft components", *Progress in Aerospace Sciences*, Vol. 34, pp. 481-541.

Leister, H-J. and Perić, M. (1994), "Vectorized strongly implicit solving procedure for a seven-diagonal coefficient matrix", *Internal Journal of Numerical Methods for Heat and Fluid Flow*, Vol. 4, pp. 159-72.

Masoudi, M. and Sirignano, W.A. (2000), "Collosion of a vortex with a vaporizing droplet", *International Journal of Multiphase Flow*, Vol. 26, pp. 1925-49.

Menter, F.R. (1994), "Two-equation eddy-viscosity turbulence models for engineering applications", *AIAA Journal*, Vol. 32 No. 8, pp. 1598-605.

Park, J-K. and Farrell, P.V. (1990), "Numerical study for free stream turbulence effects on a single droplet vaporization", SAE Technical Paper Series, 901607.

Patankar, S.V. (1980), *Numerical Heat Transfer and Fluid Flow*, Hemisphere Publishing Corporation, New York, NY.

Prakash, S. and Sirginano, W.A. (1979), "Theory of the convective droplet vaporization with unsteady heat transfer in the circulating liquid phase", *International Journal of Heat and Mass Transfer*, Vol. 23, pp. 253-68.

Ranz, W.E. and Marchall, W.R. Jr (1952), "Evaporation from drops", *Chemical Engineering Progress, Part II*, Vol. 48, pp. 173-80.

Sundararajan, T. and Ayyaswamy, P.S. (1984), "Hydrodynamics and heat transfer associated with condensation on a moving drop: solution of intermediate Reynolds number", *Journal of Fluid Mechanics*, Vol. 149, pp. 33-58.

van Doormall, J.P. and Raithby, G.D. (1984), "Enhancement of the simple method for predicting incompressible fluid flows", *Numerical Heat Transfer*, Vol. 7, pp. 147-63.

Wu, J-S., Lin, Y-J. and Sheen, H-J. (2001), "Effects of ambient turbulence and fuel properties on the evaporation rate of single droplets", *International Journal of Heat and Mass Transfer*, Vol. 44, pp. 4593-603.

Zhang, H. (2003), "Evaporation of a suspended droplet in forced convective high-pressure environments", *Combustion Science and Technology*, Vol. 175, pp. 2237-68.

Zhou, J. and Liu, J. (2004), "Numerical study on 3-D light and heat transport in biological tissues embedded with large blood vessels during laser-induced thermotherapy", *Numerical Heat Transfer A*, Vol. 45, pp. 415-49.

Corresponding author
Madjid Birouk can be contacted at: biroukm@cc.umanitoba.ca

To purchase reprints of this article please e-mail: **reprints@emeraldinsight.com**
Or visit our web site for further details: **www.emeraldinsight.com/reprints**